Heritage Science

RESEARCH

Open Access

Cu and As containing pigments in Zhejiang architecture polychrome paintings: a case study of degradation products of emerald green

Ling Shen[1*], Chenya Wang[2], Jiachen Zhang[3], Biao Cui[3], Suimin Zhu[3] and Jianqiang Mao[4]

Abstract

The discoloration of pigments caused by deterioration may significantly alter an artifact's original pattern and design, which could have an impact on its intended meaning. The green pigments containing copper (Cu) and arsenate (As) in paintings are usually recognized as Emerald green or Scheele's green and are also infrequently reported as cornwallite and lavendulan. Recent studies point out that lavendulan may be the degradation product of Emerald green but not a natural mineral. Overall, there are still relatively few cases of current studies on green pigment with Cu and As. The elemental composition and molecular structure of green minerals containing Cu and As are similar, so it is difficult to identify by Raman spectroscopy. The green pigment samples used in this investigation were taken from architectural paintings in the Wenchang palace and traditional Ziweishan dwellings. The composition of the paint samples was investigated comprehensively by Raman spectroscopy, scanning electron microscope observation, micro-X-ray diffraction (μ-XRD), X-ray photoelectron spectroscopy (XPS) and X-ray absorption near-edge spectroscopy (XANES) analysis. From the results of elemental distribution, the pigments mainly contain Cu, As, and Cl. The morphological results illustrated that the particles in these three pigments are rounded and granular, indicating the synthetic pigment is possibly emerald green. The characteristic vibrational peaks of the As–O, Cu–O and Cu–Cl bond were detected by Raman spectroscopy, and infrared spectroscopy found the presence of oxalate salt. The XPS and XANES analysis results show that As valence is + 5. This study found that the green pigment samples are a degradation product of emerald green. The formation of this product is related to the preservation environment. The results of this work will provide information to understand the degradation processes of emerald green and be a reference for the identification of pigments containing Cu and As elements.

Keywords Architecture Painting in Zhejiang Province, Pigment, Emerald green, Degradation

Background

In archaeology and art history, color is one of an object's most crucial characteristics, and when a pigment becomes discolored, the original design and meaning of the artifact may change. Green pigments containing copper (Cu) are mostly copper compounds [1]. More research has been carried out on the mechanisms for the discoloration of copper-containing pigments such blue bronze ore, malachite, and verdigris [2, 3]. Along with these common pigments, the synthetic pigment Emerald green's color-changing process has also gained attention recently.

*Correspondence:
Ling Shen
shenling@zucc.edu.cn
[1] Archaeology Department, Hangzhou City University, Hangzhou 310015, Zhejiang, China
[2] Hangzhou Municipal Institute of Cultural Relics and Archaeology, Hangzhou 310000, Zhejiang, China
[3] Zhejiang Provincial Institute of Cultural Relics and Archaeology, Hangzhou 310007, Zhejiang, China
[4] Jiangshan Culture Radio Film and TV Tourism Administration, Quzhou 324100, Zhejiang, China

The synthetic pigments Emerald green ($3Cu(AsO_2)_2Cu(CH_3COO)_2$) and Scheele's green ($Cu(AsO_2)OH$) are typically Cu and As included green pigment [4]. Emerald green was invented between 1798 and 1814 AD and was used extensively in architectural painting and drawings in China since the late Qing dynasty (After 1890s AD) [5–7]. Scheele's green, the first known synthetic Cu and As pigment, was created in 1775 but was later supplanted by Emerald green due to its high level of toxicity [8]. As a result, there are more reported cases of cultural heritage in Emerald green than in Scheele's green. Since the twentieth century, China's architectural paintings have heralded a widespread use of emerald green.

Recently, concerns of Emerald green discolouration are starting to surface. In the case of oil painting, Emerald green form copper palmitate and arsenic trioxide in normal light and temperature, which results in the color change from green to brownish [9]. Additionally, it has been noted that regions that were painted Emerald green can turn brown because the pigment can react with hydrogen sulfide in the air to generate black CuS [10]. Compared to malachite, azurite, and other pigments containing copper, emerald green is more likely to pose a health hazard since it contains arsenic. Studies have reported that arsenic oxide is slightly soluble in water and is distributed in a pentavalent mainly As(V) in the entire pigment layers [11]. In addition, A recent study discovers that emerald green along with lavendulan in the same area has been reported in several studies. Accordingly, some academics have hypothesized that lavendulan may be formed as a consequence of Emerald green's degradation [12–14]. Another report is mural painting in Iran, in an acid environment triggers the reaction of Cu^{2+} and arsenate ions, leading to the formation of lammerite [15].

Chen reported that, in the late 20th-century architectural painting located in Zhejiang, conichalcite ($CaCuAsO_4(OH)$) was detected by Raman spectroscopy mainly depending on the main peak [16], which has not been reported as a pigment in other cultural heritage sites. Zhejiang's humid climate makes it challenging to preserve architectural paintings, particularly those on a wooden base. As a result, there are relatively few architectural polychrome paintings overall. The existing ones are mainly Jiangnan dwelling buildings from the morning of the late Ming and Qing dynasties (After the seventeenth centuries). Cornwallite ($Cu_5(AsO_4)_2(OH)_4$), a natural mineral pigment that contains copper and asteroids, has been used historically and can be traced to the Song dynasty (between the tenth centuries—13rd C centuries AD) and Pompeii period, periods that are equivalent to those before the creation of Emerald green [17, 18]. Therefore, conichalcite may be either a unique ore found only in that area, which is a new color, or Emerald green's ageing caused its formation.

To clarify this problem, in this current study, the samples are collected from the architectural paintings located in Kaitai Hall (开泰堂), Ziweishan traditional dwelling (紫薇山民居) in Jinhua and Wenchang Palace (文昌宫) (destroyed in the Ming Dynasty and rebuilt in the Qing Dynasty at 1909) in Jiangshan. Both of the architectural locations are in Zhejiang Province (Fig. 1a, b), which has abundant rainfall and moist air throughout the year. The district where Wenchang Palace is situated at 101.21 m above sea level and has a humid subtropical, no dry season climate. Dongyang, where Ziweishan traditional dwellings is located, also has a humid subtropical climate with an an average rainfall of 203–230 mm [19, 20]. The green color in Wenchang Palace was lighter, it was impossible to tell only by visual observation alone whether the hue change was due to discoloration, flaking or an initial mixture with white pigment. The prior In-situ nondestructive investigation with p-XRF found Cu and As in green and blueish-green areas. The green-colored section that displayed evident flakes from the painting was chosen as the sampling point to do further analysis to determine the chemical compositions of the green pigments. We conducted a micro-area analysis of three green and blue-green samples containing Cu and As from the Kaitai Halls, Ziweishan traditional residence, and Wenchang Palace paintings. Samples were labelled KKT, WCG-1, and WCG-2. The KKT is obtained from the painted lower purlin on the 5-purlin beam on the western side in the Kaitai Hall, the main hall of Dafudi; WCG-1 is taken from the window frame to the south on the third floor, and WCG-2 is sampled from the painted ceiling on the third floor near the south window (Additional file 1: Figure S1). The specific sampling location is illustrated in Fig. 1b, c, d. The analytical methods employed in this study are: micro-Raman spectroscopy (μ-RS), scanning electron microscopy coupled with energy dispersive Xray analysis (SEM–EDX), micro-Fourier Transform Infrared Spectroscopy (μ-FTIR), X-ray diffraction analysis (XRD), X-ray photoelectron spectroscopy, and microscopic X-ray absorption near-edge spectroscopy (μ-XANES) analysis.

Experimental

Due to the tiny sampling quantity, the experiments were performed follow the order from nondestructive to destructive steps, starting with microscopic observation, XRD and XPS analysis, In the case if the specific pigment could not be determined, further elemental SEM–EDS, micro-Raman spectroscopy, XANES analysis was performed after embedding the samples. The methods and parameters are listed as follows and the folw chart is shown in Fig. 2.

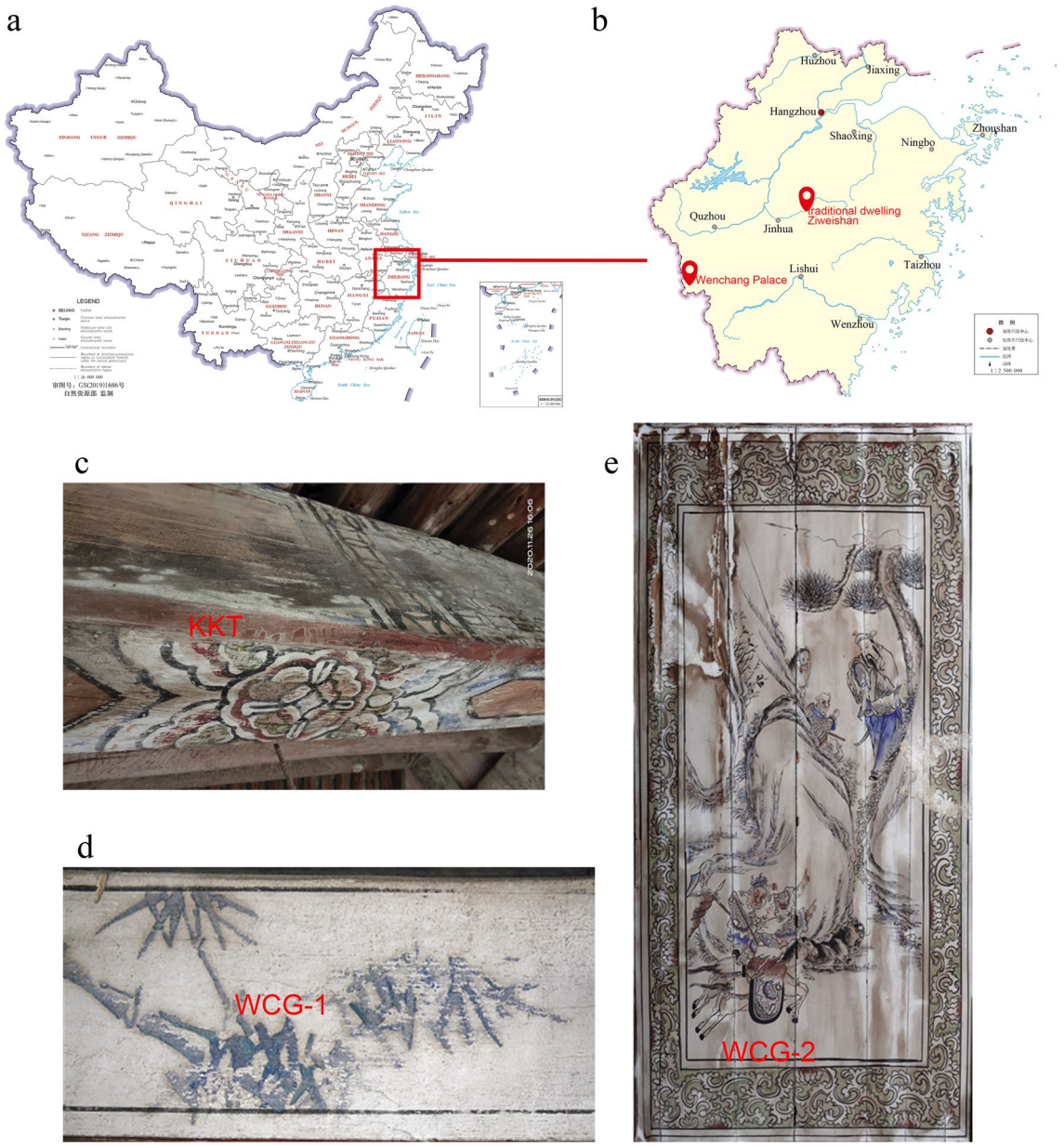

Fig. 1 Location of the architecture and sampling. **a** Location of Zhejiang Province within China and **b** the location of Wenchang palace, and Ziweishan traditional dwelling in Zhejiang Province; **c**–**e** Sampling locations of KKT, WCG-1 and WCG-2

Optical microscopy

All painting samples and embedded cross-section were observed by a KEYENCE VHX-5000 ultra depth of field 3D video microscope. The magnification was set ranging 200–1000X.

XRD

The samples (paint side face up) were directly measured by Rigaku Dmax-2500 X-ray diffractometer with a Cu target source, at 40 kV voltage and current of 100 mA. The scanning range was 5° to 80°, and the scanning speed was 10°/min. The data were analyzed by MDI jade 6.0 software.

Embedding

The samples were embedded in cold inlay epoxy resin and dry polished with Micro-mesh® polishing cloths to the final step of 12000# mesh.

SEM–EDX

Scanning electron microscopy in combination with energy dispersive X-ray analysis (SEM–EDX) studies was

performed at a low vacuum mode (20 pa) by Phenom XL with an EDX system with spot/region analysis and elemental mapping facilities. Backscattered electron (BSE) images of the cross-sections were taken at a 15 kV accelerating voltage. The magnification was set ranging 200–5000×.

μ-RS

Micro-Raman Spectroscopy was performed on embedded sample on cross-section surface to qualitatively analysis the composition of green pigment. Thermo Scientific DXR 2xi Micro-Raman spectrometer with 532 nm laser was applied on the experiment. The spectral range is 100–1500 cm^{-1}, and the collection time was 2–10 s, the accumulation time is 3 times.

μ-FTIR-ATR

The FTIR spectral data were collected on Bruker LUMOS II FTIR spectrometer combined with a germanium crystal was used for attenuated total refraction (ATR) analysis and 16 × 1pixel linear mercury cadmium telluride (MCT) array detector for imaging. The spectral range of 4000–800 cm^{-1}, at a spectral resolution of 4 cm^{-1}.

XPS

A Thermo Scientific ESCALAB 250Xi X-ray photoelectron spectrometer was used for the analysis of the binding energy of the As 3ds. Analysis was performed with an X-ray beam of around 200–900 μm and the source of monochromatized Al–Kα (hm = 1486.6 eV), vacuum 5×10^{-8} Pa, nitrogen atmosphere, and optimal spatial resolution below 20 microns. The binding energy of C 1 s (284.8 eV) was used as the internal reference. XPS PEAK41 software was applied for analyzing XPS data.

μ-XANES

The experiment was carried out on cross-section sample KKT and WCG-1 at beamline BL15U1 of the SSRF to confirm and refine the results obtained at XPS analysis. X-ray absorption spectroscopy operated at an energy range from 11.817–12.017 keV (Fig. 2).

Result

Optical observation

Figure 3 shows the microscopy observation pictures of the three samples, where Fig. 3d–f are 1000× magnification pictures. Figure 3a and d demonstrate that the average of the green pigments in KKT is dark green, with the dark hue primarily appearing in the sample's upper layer. Figure 3b and e clearly illustrate that WCG-1 is a blue-green pigment mixed sample, and the green particles in WCG-2 appear relatively light green (Fig. 3f). The green pigment particles in the three samples are all about 10 μm in size.

XRD analysis

Figure 4 represents the results of XRD analysis of the painting fragment placed directly on the single crystal silicon wafer (data including the earth round layer and white ground layer). The two samples from Wenchang palace, WCG-1 and WCG-2 owned similar spectral patterns. It shows that the white ground layer of the samples is mainly calcite ($CaCO_3$), while the white ground layer of the KKT is calcium sulfate (Gypsum, $CaSO_4$). The gypsum found in the WCG-1 and WCG-2, was probably produced when the SO_2 in the air dissolved in rainwater, forming sulfuric acid and sulfite, which subsequently reacted with the $CaCO_3$ in the ground layer. The presence of calcium oxalate (Weddellite, CaC_2O_4) in all samples possibly results from the oil and animal glue that the main binder contained. Oil and animal glue are inclined to breed microorganisms and generate organic acids, which would react with the calcareous substrate to form calcium oxalate. Additionally, vaterite, a mineral most frequently found in the nacre of mollusks, is discovered in the materials from the Wenchang palace. The presence of vaterite suggests that shells were likely pulverized into

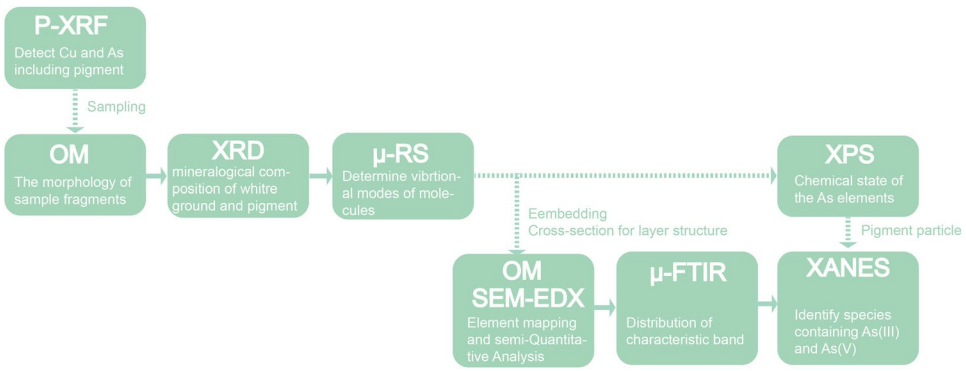

Fig. 2 Flow chart of the experimental

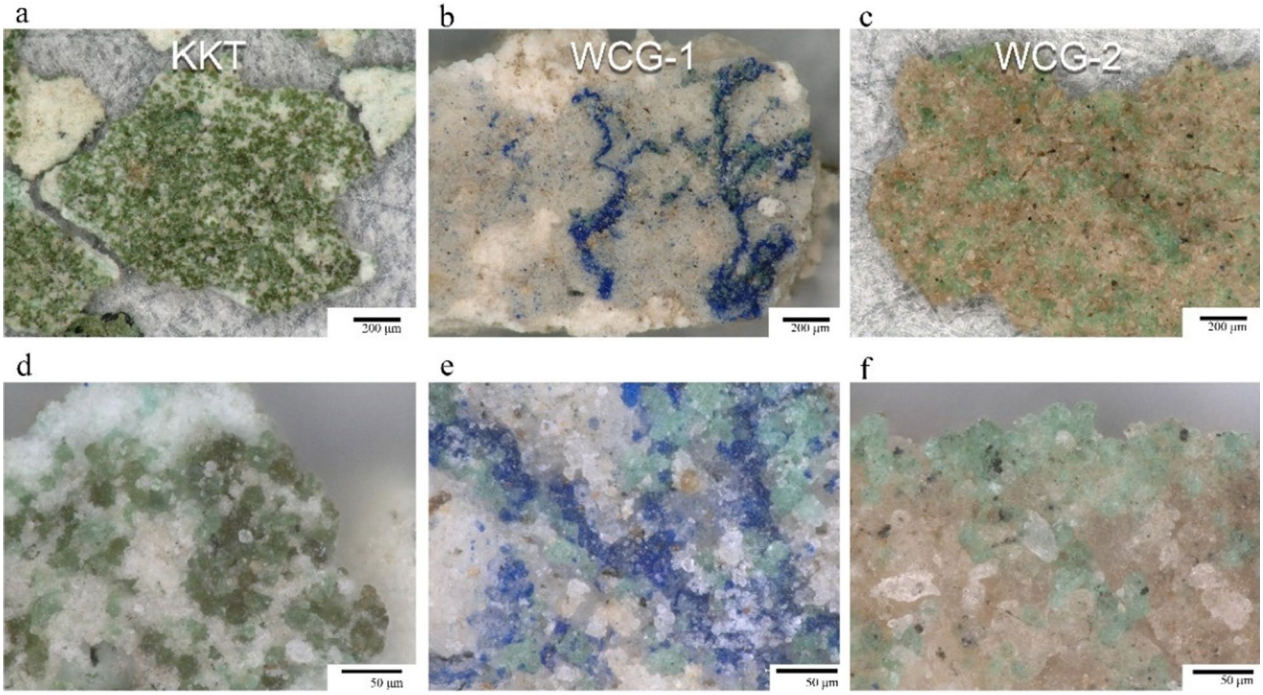

Fig. 3 The morphology of sample fragments under different magnification. **a**–**c** are the sample surface morphology under 200× magnification; **d** and **f** are the samples of green particles under 1000× magnification

a fine powder to act as the white pigment for the white ground layer. Barite ($BaSO_4$) is also detected from the WCG-2.

However, we had difficulty identifying the Cu and As compounds' peaks because the tiny quantity of the green pigment sample was below the lower band. As a result, the next step was to operate a micro-area analysis to determine the pigments' molecular structure and elemental composition.

μ-RS

The results of μ-RS analyses of pigments in each pigment layer are shown in Fig. 5. In Fig. 5, the Raman spectra of the three green pigments samples from Kaitai Tang (KKT) and Wenchang palace (WCG-1, WCG-2) show relatively consistent peaks, which suggests each green pigment should composite of the same substance, with intense peaks mainly at 825–835 cm^{-1}, and peaks near 330 cm^{-1}. The Raman spectra of the samples differ from the reported Raman spectra of Emerald green [14], implying that the substance is not Emerald green. Comparison with the published Raman spectra of green pigments containing Cu and As reveals similarity to the characteristic signals of conichalcite ($CaCuAsO_4(OH)$) [16]. Ref. [16] shows similar result as this Raman spectroscopy measurement, KKT, WCG-1 and WCG-2 illustrate main peak at 822 cm^{-1} that is consistent with conichalcite. Nevertheless, still found to be off around 400–500 cm^{-1} and below 200 cm^{-1}, so the green pigment cannot be identified as conichalcite only by the main peak. The possibility of cornwallite ($Cu_5(AsO_4)_2(OH)_4$) and lavendulan ($NaCaCu_5(AsO_4)_4Cl\text{-}5H_2O$) thus could be refuted. The peaks at 979–980 cm^{-1} is corresponding to the stretching vibration of OH^-, and the peaks near 840–850 cm^{-1} and 610 cm^{-1} correspond to the stretching vibrations of As–O. The peaks below 600 cm^{-1} are mainly attributed to the Cu–O and Cu–Cl [21]. Considering the pigment's era (the twentieth century) and the small particle size, it should be artificial ultramarine. Thus, the blue-green color in WCG-1 can be attributed to a combination of blue ultramarine and this copper arsenate pigment.

SEM–EDX analysis

The cross-section of the samples is shown in Fig. 6. From the results of elemental mapping in Fig. 6g–s, it can be seen that Cu, As and Cl in the green pigment is distributed in the same place, indicating that the green particles contain Cu, As and Cl. Additionally, as seen in Fig. 6p–s, the element Ca primarily remained at the outer edge of particles. This finding could lead to the hypothesis that Ca leaches into the green pigment from the external circumstance; Ca is thereby only adsorbed on the surface rather than being involved in the crystal formation. In this case, Ca is highly likely to originate from the white

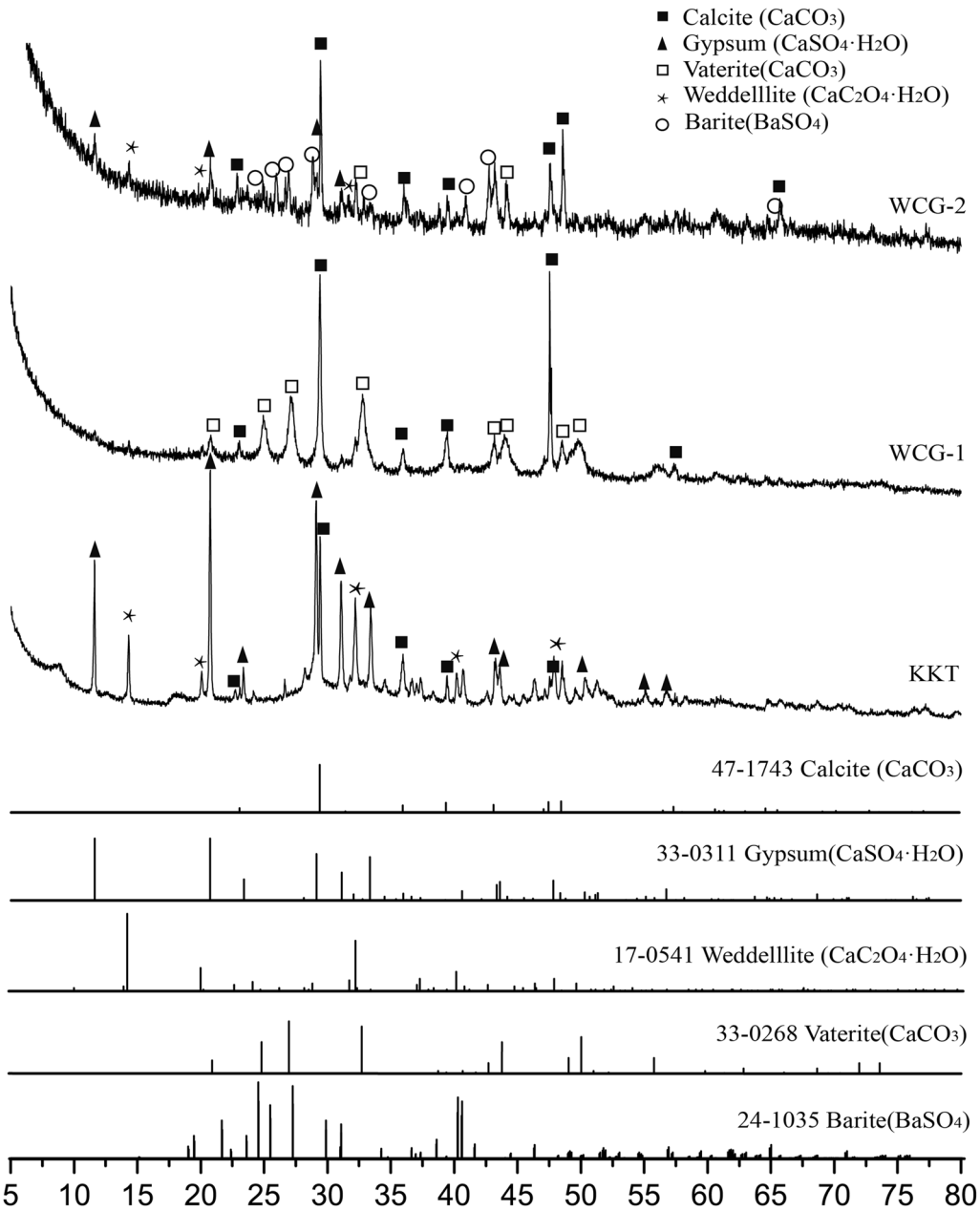

Fig. 4 XRD spectra and identify results

ground base, due to the dissolution of acid rain, Cl_2, SO_2, NO_2 and the oxalic acid caused by the dissolution of calcium-containing materials, and the calcium ions migrate to the top of pigment layer with evaporation and adsorbed to the green particles.

Figure 6a shows that the pigment morphology is rounded and granularly cracked, which indicates that it is a synthetic pigment. From the BSE image of the particle magnified at 5000× in Fig. 6, it can be seen that the elemental distribution inside the particle is not uniform, where the brighter part is the As due to its higher atomic mass. The morphology of the green pigment particles is more similar to that of emerald green [14]. Judging from the standpoint of crystal morphology, the green pigment used at that time was presumably emerald green, which underwent different degrees of degradation. According to

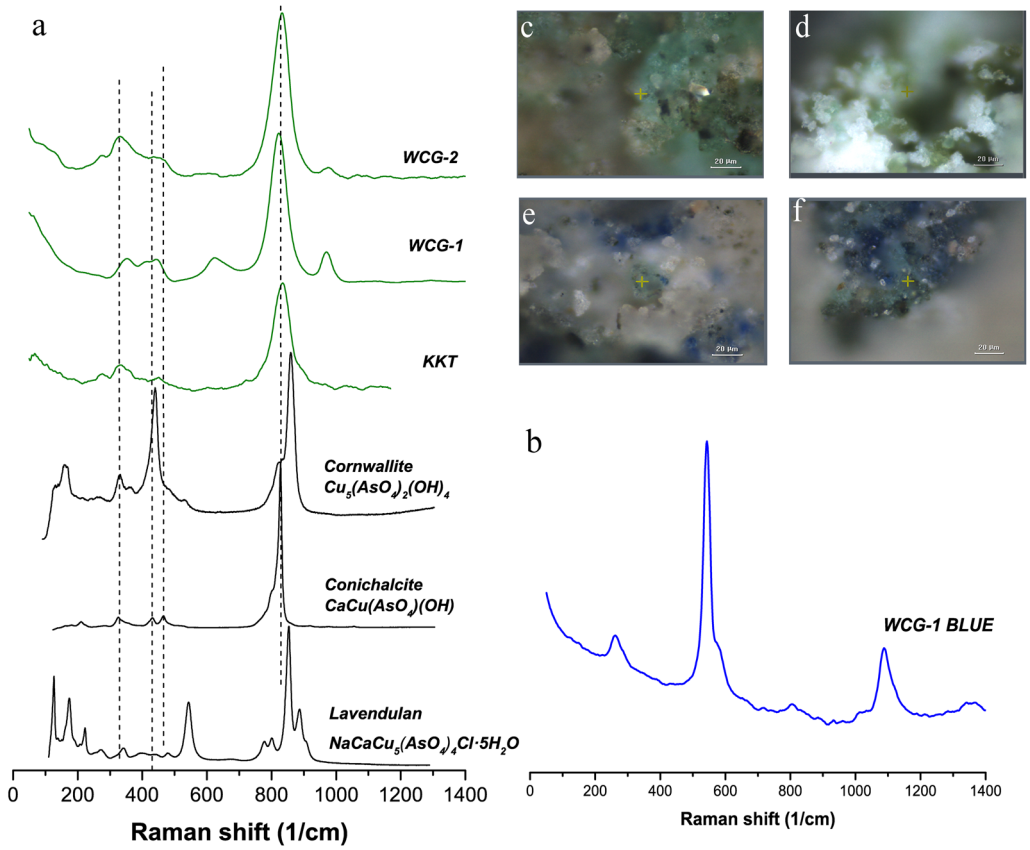

Fig. 5 Raman spectra and the measure point. **a** Raman spectra of green pigments from KKT, WCG-1 and WCG-2 and the reference standard spectra from RRUFF; **b** the Raman spectrum of the blue pigment in WCG-1; **c** the measurement point for green particle in KKT; **d** for green particle in WCG-1, **e** for WCG-2, **f** is for blue pigment in WCG-1

the quantitative results of region analysis in Table 1, the elemental compositions of the three samples are similar. The concentration of Na is comparably low, suggesting that the particles cannot be $NaCaCu_5(AsO_4)_4Cl\text{-}5H_2O$, a degradation product in the literature [12, 14]. The results of EDX also indicate that the element composition in several samples is relatively close to each other. The atomic concentration proves that the atomic ratio of Cu: As in the particle is near 5:3 to 5:4, the change is because the distribution of As in the particle is uneven Fig. 7c. The atomic ratio of Cu:Cl is about 5:1. The content of Ca in sample KKT is relatively low, with an atomic ratio of Cu:Ca of about 2:1, while the sample Cu:Ca ratios in samples WCG-1 and WCG-2 reach 5:4 to 1:1. The higher Ca concentration is likely to contribute to the whitish color of the green particle, shown by WCG-2. Even though Ca is detected in the particles, Fig. 6p, q, s suggest that calcium and copper do not occur in the same compound so that the green pigment cannot be conichalcite.

μ-FTIR-ATR

μ-FTIR-ATR analysis of samples identified CaC_2O_4 in all samples, $BaSO_4$, and $CaCO_3$ in samples WCG-1 and WCG-2, gypsum in KKT, and ultramarine as the blue pigment in WCG-1, which agrees with the SEM–EDX, XRD, and μ-Raman spectroscopy results.

The absorption at 870 cm^{-1} (C–O out of plane bending) is utilized to map calcium carbonate distribution, while the band at 1110 cm^{-1} is used to map gypsum distribution. Ultramarine is identified by a broad peak at 990 cm^{-1}; $BaSO_4$ is confirmed by a band at 1074 cm^{-1} [22].

The characteristic band at 787 cm^{-1} (Fig. 8d–f) is used to map the distribution of the green pigment, which is attributed to As–O stretching vibration [23, 24]. Peaks at 1621 cm^{-1} (Vas COO–) and 1318 cm^{-1} (Vs COO–) were discovered in the spectra of Cu and As, which were most likely due to oxalate slat. The oxalate distribution is plotted by the band at 1318 cm^{-1}. $H_2C_2O_4$ may originate from

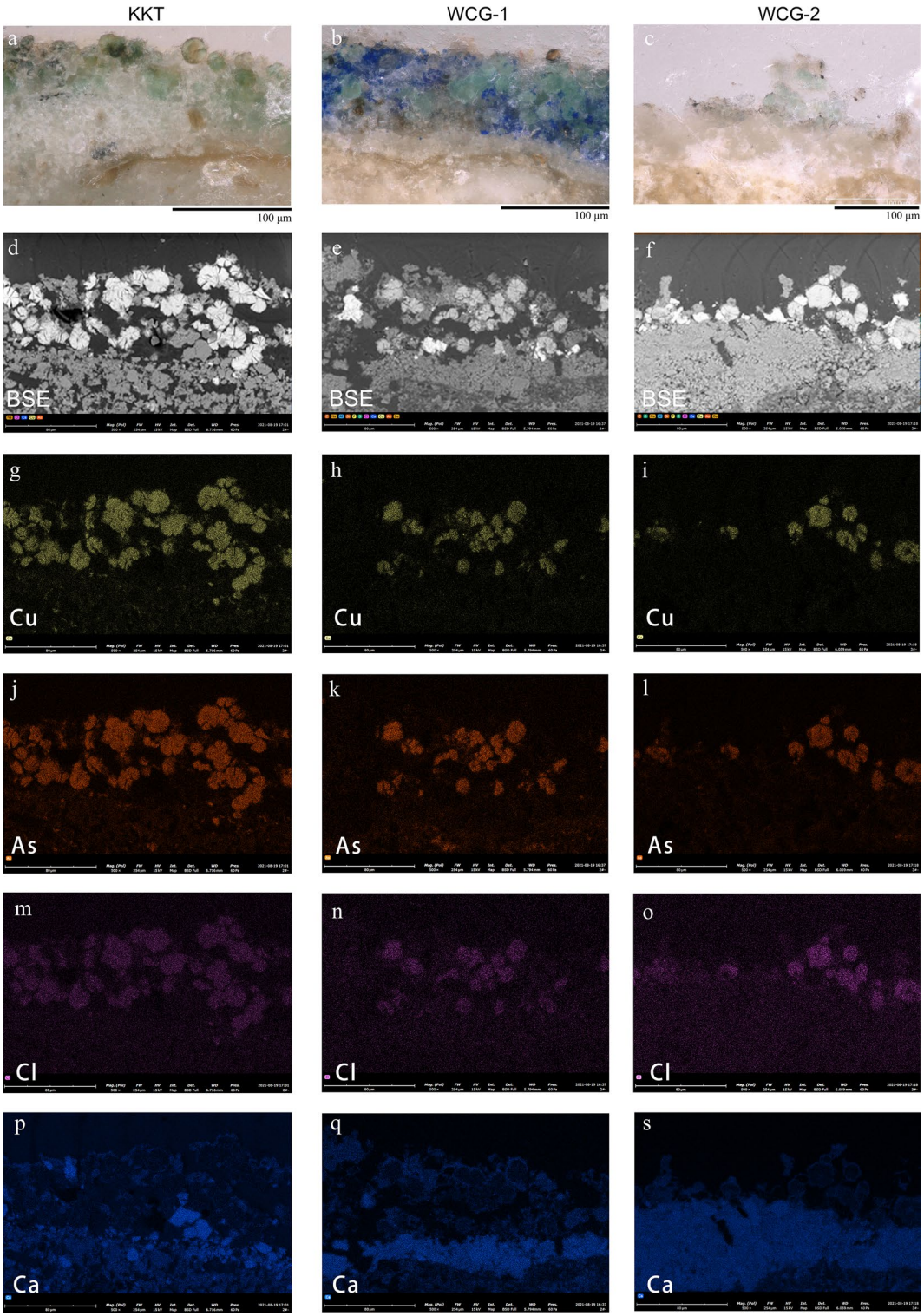

Fig. 6 Cross-section of the samples and the element mapping. **a**–**c** are the optical micro-morphography; **d**–**f** the BSE images and **g**–**s** the EDX maps of Cu, As, Cl, Ca elemental distribution images

Table 1 The quantitative analysis results with SEM–EDS of green pigments in samples

Atomic Conc. %													
Sample	**C**	**O**	**Na**	**Mg**	**Al**	**Si**	**P**	**S**	**Cl**	**K**	**Ca**	**Cu**	**As**
KKT	47.6	37.1	0.2	0.0	0.1	0.1	0.1	0.2	1.2	0.4	3.2	6.2	3.8
WCG-1	45.6	38.2	0.4	0.0	0.4	0.4	0.1	0.7	1.0	0.2	4.0	5.5	3.6
WCG-2	44.7	39.2	0.2	0.1	0.2	0.3	0.0	1.0	1.0	0.2	5.1	4.9	3.2

microbial metabolites or the oxidation of organic binding media [25]. The infrared spectrum of copper oxalate is characterized by the formation of distinct bimodal peaks near 1319–1363 cm^{-1} [26, 27]. Because no distinct double peak was seen in this spectral region (Fig. 8q, s), the oxalate is most likely calcium oxalate rather than copper oxalate. According to the distribution maps, the band at 1318 cm^{-1} belonging to the CaC_2O_4 band at 1318 cm^{-1} is distributed at or around the green pigment (band at 787 cm^{-1}). Furthermore, gypsum is scattered over the painting layer, particularly in the top layer of all samples.

Elemental valence of As

XPS analysis

To further determine the chemical state of the As elements in the pigments, three pigment samples were investigated by X-ray photoelectron spectroscopy. As the results (Fig. 9) revealed, the spectra of the three samples were similar. The major binding energy of As $3d_{3/2}$ was around 44.5 eV, besides the binding energy of As $3d_{3/2}$ was 44.9 eV, which is close to the binding energy of Na_3AsO_4 in the Nist spectral library [28] and As(V) reported in the literature [29], suggesting that arsenic might be present as As(V). The binding energy of As $2p_{3/2}$ was around 1326.8 eV. The value is consistent with the binding energy of As(V) reported in the database and the literature [10], indicating that arsenate (As^{5+}) compounds are present in all three samples.

XANES

K-edge XANES analyses carried out on the KKT and WCG-1 sample to identify species containing As(III) and As(V). Figure 10 illustrates the XANES result taken from the green particles in the top part of the pigment layer and Na_2HAsO_4 $7H_2O$ (Sigma–Aldrich) applied as a reference of arsenate (As^{5+}). Compared with the reference, the white line of CuAs rich green particle is found at 11,872.5 eV, matching the reference arsenate (As^{5+}). The white line energy is not high as the arsenic trioxide, which is reported as 11,975.4 eV in reference library [11]. This result shows that copper or calcium arsenates probably present as arsenic degradation products instead of arsenic oxide.

Discussion

No arsenate-containing pigments such as orpiment (As_2S_3) and realgar (As_4S_4) are found in the surroundings of the painting layer, so it can be excluded that As does not come from the migration from the surrounding pigments but is present in the original pigment. From the morphological characteristics of the circular shape with multi-cracks (Fig. 8), the sample investigated in this study should originally be the synthetic green pigment Emerald green. The characteristic peaks of Emerald green cannot be found in the Raman and FTIR spectra of the green pigment samples, indicating that Emerald green has completely degraded and transformed into a new compound.

The results of EDX analysis show that the ageing product of the pigment contains a high content of Ca, and the distribution of Ca in the elements is uneven (Fig. 6p, q, s), which indicates that the ageing product is a mixture, not conichalcite, and the IR spectrum shows that it may contain CaC_2O_4. The source of Ca is speculated to be the white ground layer, due to the high humidity and acid rain in southern China, which is easy to cause Ca^{2+} formation, with the reaction formula as Eqs. (1)–(3). the white ground layer of KKT is mainly calcium sulfate, which has relatively lower solubility than calcium carbonate in acid, and also consequently releases comparably fewer Ca ions formed. Therefore, the concentration of Ca in the green pigment of KKT is relatively low (Table 1).

$$2SO_2 + O_2 \rightarrow 2SO_3 \tag{1}$$

$$SO_3 + H_2O \rightarrow 2H^+ + SO_4^{2-} \tag{2}$$

$$CaCO_3 + 2H^+ \rightarrow Ca^{2+} + H_2O + CO_2 \tag{3}$$

Rare studies are focusing on the ageing process of Emerald green. As to oil painting, the darken phenomena has been reported and investigated. Katrien Keune analyzed emerald green pigments in oil paintings by infrared spectroscopy and found the generation of copper palmitate and arsenic trioxide, which leads to the darkening of oil paintings under light conditions [9]. In 2016, they focus on the change of As and indicated that the most likely ageing product of arsenic-containing pigments is arsenate; furthermore, arsenate ions are easily adsorbed

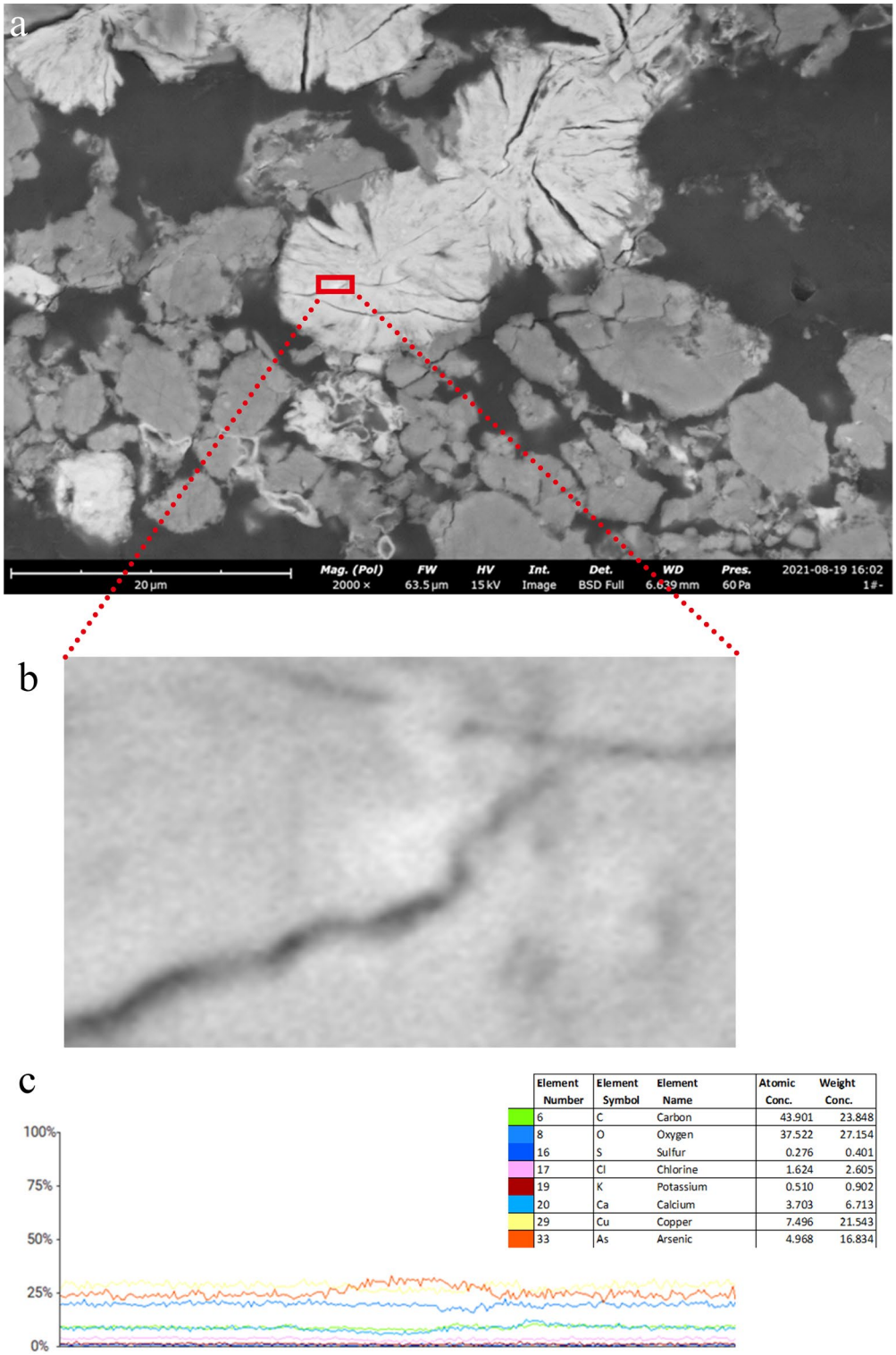

Element Number	Element Symbol	Element Name	Atomic Conc.	Weight Conc.
6	C	Carbon	43.901	23.848
8	O	Oxygen	37.522	27.154
16	S	Sulfur	0.276	0.401
17	Cl	Chlorine	1.624	2.605
19	K	Potassium	0.510	0.902
20	Ca	Calcium	3.703	6.713
29	Cu	Copper	7.496	21.543
33	As	Arsenic	4.968	16.834

Fig. 7 Pigment particle and line scan elemental analysis. **a** Magnification of pigment particles in KKT samples and **b** Cut out of line scan and **c** the combined line scan elemental analysis (The red frame is the measurement area)

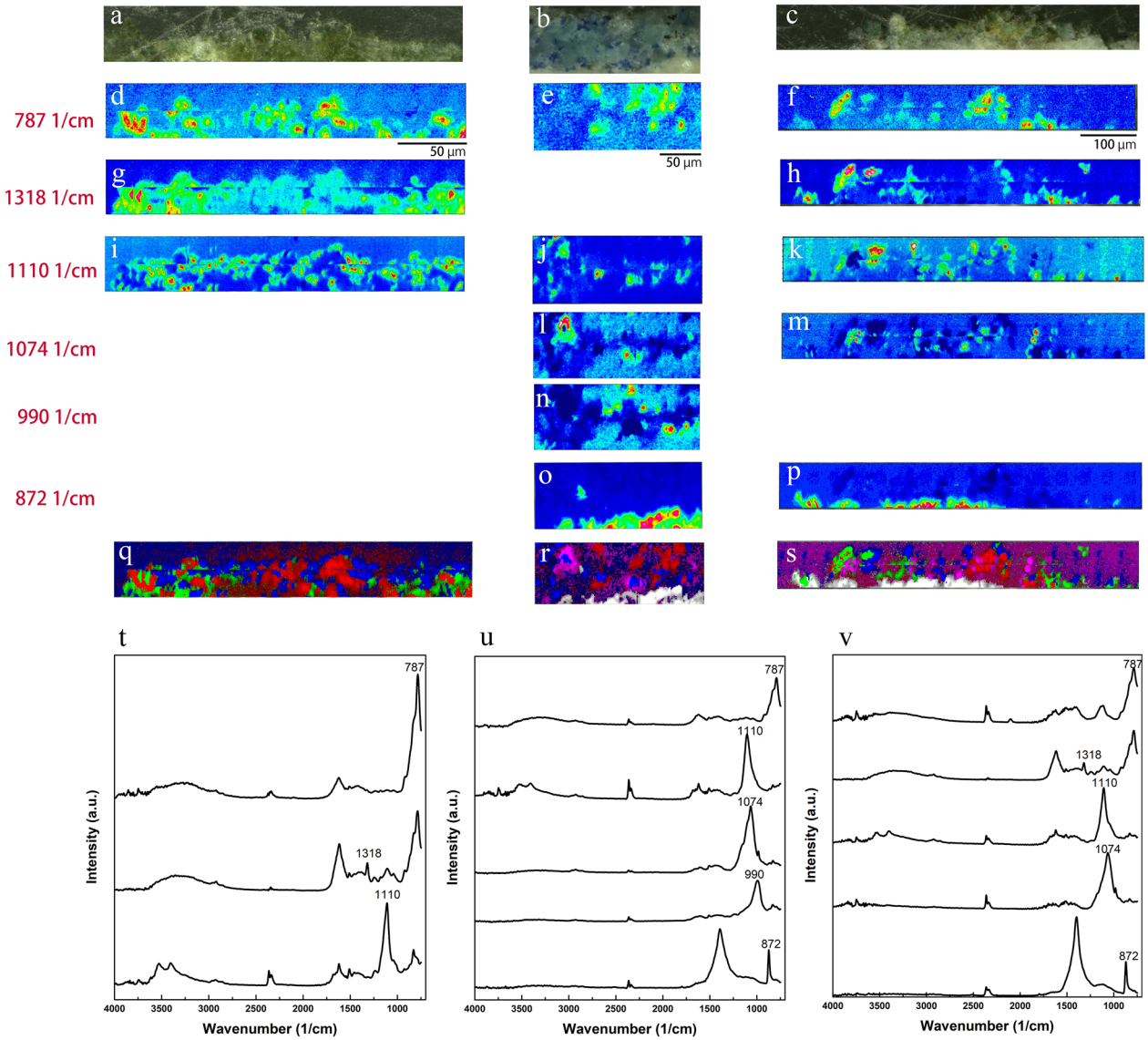

Fig. 8 False color-plots μ-FTIR-ATR images and the characteristic spectra. **a**–**c** The measurement location; **d**–**p** the distribution maps of 787 cm^{-1}, 1318 cm^{-1}, 1110 cm^{-1}, 1074 cm^{-1}, 990 cm^{-1}, 872 cm^{-1} in three samples; **q**, **r**, **s** the image segmentation of different distribution maps of characteristic peak; **t**–**v** the representative FTIR-ATR spectra belonging to each band distribution maps

on Pb and Ca atoms [11]. Zhimin Li pointed out that lavendulan was the degradation product of emerald green under salt-containing conditions and underground water probably be the origin of Cl salts [14]. In contrast, the ageing products reported in the above studies were not the same as the pigments in this study.

A specific concentration of Cl was also detected from the green pigment particle by SEM–EDX analysis, suggesting that Cl adsorb to the particle and leads to emerald green transforming into another copper arsenate compound. According to Table 1, the atomic ratio of Cu, As and Cl is close to 5:3:1. The Cl may mainly come from the frequent acid rain in the environment. In addition, the As in arsenate compounds is present as As(V), indicating that the pigment particles have completely oxidized during the ageing process. The XPS result shows arsenic present as As^{5+}, and the degradation product may follow the molecular formula: $Cu_5(AsO_4)_3Cl\ xH_2O$. Ca is not involved in crystal formation, but formed mainly around the green pigment in the form of calcium oxalate.

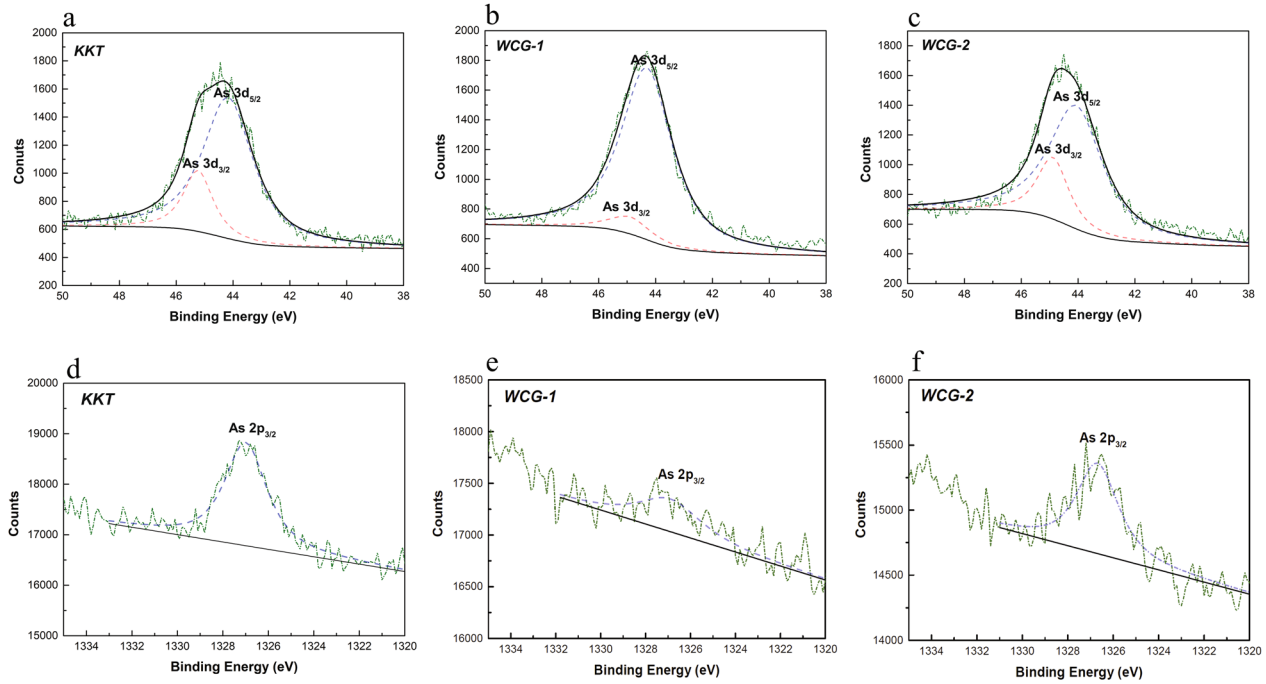

Fig. 9 XPS results of As in the green pigment. **a**–**c** the binding energy of As $3d_{3/2}$ in samples KKT, WCG-1 and WCG-2; **d**, **e** and **f** the binding energy of As $2p_{3/2}$ in samples KKT, WCG-1 and WCG-2

The difference in the reaction products may be because Zhejiang architectural painting is restored mainly in an acidic and humid environment. The formation process of this ageing product is inferred as follows:

$$Cu(C_2H_3O_2)_23Cu(AsO_2)_2 + H^+ \rightarrow Cu^{2+} + {AsO_2}^{2-} + CH_3COO^- \quad (4)$$

$$AsO_2{}^{2-} + H_2O + O_2 \rightarrow AsO_4{}^{3-} + H^+ \quad (5)$$

$$CaCO_3 + 2H^+ \rightarrow Ca^{2+} + H_2O + CO_2 \quad (6)$$

$$H_2C_2O_4 + CaCO_3 + H_2O \rightarrow CaC_2O_4 \cdot 2H_2O + CO_2 \quad (7)$$

$$Cu^{2+} + AsO_4{}^{3-} + Cl^- + H_2O + O_2 \rightarrow Cu_5(AsO_4)_3ClXH_2O \quad (8)$$

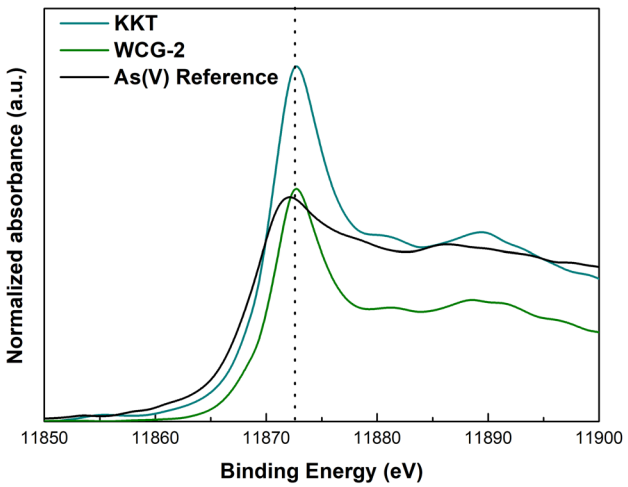

Fig. 10 Arsenic -K-edge XANES spot analysis results. The dotted line indicates the white line for As(V)

The Emerald green ageing products in the Dazu stone carving statue painting are lavendulan, because where both emerald green and lavendulan were found in the green pigment of the small Buddha Bay statue in Dazu Baoding Mountain, and calcium oxalate was also detected [30]. Considering the environment of Dazu grottoes, researchers believe that the degradation progress of emerald green may have been promoted by water-salt as well as acidic media conditions. In contrast, unlike the previously investigated cultural heritage sites in China, where most of the previously reported lavendulan cases occurred in cave-temple. However, the source of Cl in Zhejiang should be mainly atmospheric rather than groundwater but the medium is still required for further research. From the analytical phenomena, the enrichment of chloride ions is the same, but the migration of arsenate ions is found in several papers [14, 29], while in the present study, the migration of As. In addition, the phenomenon the color

change is not obvious as the ones in the Dazu rock carvings and the church in Yunnan Cizhong where the particle's color changes from green to blue-green. However, the samples in the present study did not undergo a color phase change, and the green color particles in Wenchang Palace are slightly whitish compared to the emerald green color. The cause of the whitened pigment is probably related to the production of CaC_2O_4 in the surface layer.

Ca enrichment around pigment particles can cause discoloration of the pigment and, in more severe cases, calcified crusting on the surface [6], which in turn makes some crack and flake peeling out of the painting surfaces. Thus, it is an issue that needs to be concerned with addressing the preventative conservation of architectural paintings in Zhejiang Province.

Conclusion

In this study, three green pigments from the Zhejiang region that contained Cu and As were examined. It should have originally been the synthetic pigment Emerald green, according to a thorough examination of the pigment's microscopic morphology. However, a crystallographic change occurred during the ageing process, resulting in a new substance containing Cu, As(V) and Cl, which is different from lavendulan previously reported in the literature as the degradation product of emerald green. The samples might be the product of emerald green ageing from the acidic rains of southern China. Calcium oxalate, another degradation consequence of the architecture painting, is discovered around the green pigment in the form of calcium.

Since the late 19th Century, emerald green has been a popular green color in ancient Chinese architecture. The study of discoloration products and the mechanism of emerald green has received little attention. Several analytical techniques were applied in this study to complement one another and provide scientific detection results, which could aid in understanding the ageing process of synthetic pigments. To verify the degradation of emerald green preserved under such environmental conditions as Zhejiang, more case studies will need to be looked at in the future, along with more precise analysis.

Supplementary Information

The online version contains supplementary material available at https://doi.org/10.1186/s40494-022-00834-y.

Additional file 1: Figure S1. The locations of each sampling points. (**a**) KKT sampled from on the 5-purlin beam on the western side in the Kaitai Hall; (**b**) WCG-1 sampled from the window frame to the south on the third floor of Wenchang Palace; (**c**) WCG-2 sampled from the painted ceiling on the third floor near the south window of Wenchang Palace.

Acknowledgements
The authors would like to thank Dr. Juan Zhang for the XANES experimental guidance.

Author contributions
LS: Methodology, Analysis, writing original draft. CW: Experimental analysis, writing—review and editing. (LS and CW contributed equally to this manuscript). JZ: Situ-investigation, experiment analysis. BC and SZ: Consulting on research content and contact experts. JM: Prapare the Situ investigation. All authors have read and agreed to the published version of the manuscript. All authors read and approved the final manuscript.

Funding
None.

Availability of data and materials
The data presented in this study are available from the corresponding author upon request.

Declarations

Competing interests
The authors declare that they have no known competing financial interests or personal relationships that could have influenced the work reported in this paper.

Received: 3 July 2022 Accepted: 18 November 2022
Published online: 13 January 2023

References

1. Avarcová S, Hradil D, Hradilová J, et al. Pigments—copper-based greens and blues. Archaeol Anthropol Sci. 2021;13(11):190. https://doi.org/10.1007/s12520-021-01406-0.
2. Lluveras A, Boularand S, Andreotti A, et al. Degradation of azurite in mural paintings: distribution of copper carbonate, chlorides and oxalates by SRFTIR. Appl Phys A. 2010;99(2):363–75. https://doi.org/10.1007/s00339-010-5673-5.
3. Wiggins MB, Heath E, Booksh KS, et al. Multi-analytical study of copper-based historic pigments and their alteration products. Appl Spectrosc. 2019;73(11):1255–64. https://doi.org/10.1177/0003702819856606.
4. Nicholas E, Valentine W, Tracey C, et al. The pigment compendium-a dictionary of historical pigments. Kidlington: A Butterworth-Heinemann; 2004. p. 149.
5. Zhang T, Kang BQ, Liu HW, et al. Analysis and study of painted pigments of Qing Palace Tibetan Qingcheng lamp corner pieces. Sci Res on Chin Cult Reli. 2020;2:88–96. https://doi.org/10.3969/j.issn.1674-9677.2020.02.016. (**in Chinese**).
6. Chen E, Zhang B, Zhao F. Comprehensive analysis of polychrome grotto relics: a case study of the paint layers from Anyue, Sichuan, China. Anal Lett. 2020;53:1455–71. https://doi.org/10.1080/00032719.2019.1709197.7.
7. Zhang C, Huang J, Zhu T, et al. Guangzhou Tongcao painting in late China Qing Dynasty (1840–1912 AD): technology revealed by analytical approaches. Herit Sci. 2021;9:9. https://doi.org/10.1186/s40494-020-00472-2.
8. Herm C. Emerald green versus Scheele's green: evidence and occurrence. In: Proceedings of the 7th interdisciplinary ALMA conference, Bratislava, Slovakia, October 17–19, 2019—Acta Artis Academica. 2020. p.189–202.
9. Keune K, Boon JJ, Boitelle R, et al. Degradation of Emerald green in oil paint and its contribution to the rapid change in colour of the Descente des vaches (1834–1835) painted by Théodore Rousseau. Stud Conserv. 2013;58(3):199–210. https://doi.org/10.1179/2047058412Y.0000000063.
10. Keune K, Boon JJ. Analytical imaging studies of cross-sections of paintings affected by lead soap aggregate formation. Stud Conserv. 2007;52(3):161–76. https://doi.org/10.1179/sic.2007.52.3.161.
11. Keune K, Mass J, Mehta A, et al. Analytical imaging studies of the migration of degraded orpiment, realgar, and emerald green pigments in

historic paintings and related conservation issues. Herit Sci. 2016;4:10. https://doi.org/10.1186/s40494-016-0078-1.
12. Cui Q, Zhang YX, Shui BW, et al. Study of copper and arsenic—containing green and blue—green pigments of rock carvings at Big Buddha Bay in Dazu. Sci Conserv Archaeol. 2020;32(6):87–94. https://doi.org/10.16334/j.cnki.cn31-1652/k.20180601236 (**in Chinese**).
13. Jiang KY, Sun YZ, Zhang ZX. A preliminary analysis of the pigments used for the Suspended Reclining Buddha in Diaoyucheng of Chongqing, China. Sci Conserv Archaeol. 2020;32(1):98–105. https://doi.org/10.16334/j.cnki.cn31-1652/k.2020.01.013 (**in Chinese**).
14. Li Z, Wang L, Chen H, et al. Degradation of emerald green: scientific studies on multi-polychrome Vairocana Statue in Dazu Rock Carvings, Chongqing, China. Herit Sci. 2020;8:64. https://doi.org/10.1186/s40494-020-00410-2.
15. Holakooei P, Karimy A, Nafisi G. Lammerite as a degradation product of emerald green: scientific studies on a rural persian wall painting. Stud Conserv. 2018;63:391–402. https://doi.org/10.1080/00393630.2017.1419658.
16. Chen EX, Zhang BJ, Lin YS, Meng CL. Research on painting pigments and binders in Murals of traditional buildings in Zhejiang Province. Orient Mus. 2018;3:107–13 (**in Chinese**).
17. Tong Y, Cai Y, Wang X, et al. Polychrome arhat figures dated from the Song Dynasty (960–1279 CE) at the Lingyan Temple, Changqing, Shandong, China. Herit Sci. 2021;9:117. https://doi.org/10.1186/s40494-021-00592-3.
18. Aliatis I, Bersani D, Campani E, et al. Green pigments of the Pompeian artists' palette. Spectrochimica Acta A Mol Biomol Spectrosc. 2009;73(3):532–8. https://doi.org/10.1016/j.saa.2008.11.009.
19. Dongyang Local Chronicle Editorial Committee. Dong yang municipal chronicles. Shanghai: Chinese Dictionary press; 1998. p. 59–62 (**in Chinese**).
20. Gao C, Pan SL, Bai ZX, et al. The influences of climate changes to Quzhou Jiangshangang's total watershed runoff. Water Science and Strategies to deal with China's Water (China) Issues-The 13rd China Water Conference Paper, Shijiazhuang, China. 2015. p. 224–229. (in Chinese)
21. Chen XL, Yang Q. Micro-Raman spectroscopy study of three green pigments containing Copper and Arsenic. Sci Conserv Archaeol. 2015;27(03):84–9. https://doi.org/10.16334/j.cnki.cn31-1652/k.2015.03.015.
22. Infrared and Raman Users Group. http://www.irug.org/. Accessed 3 Jun 2022.
23. Reddy BJ, Frost RL, Martens WN. Characterization of conichalcite by SEM, FTIR, Raman and electronic reflectance spectroscopy. Mineral Mag. 2005;69(2):155–67. https://doi.org/10.1180/0026461056920243.
24. Frost RL, Weier ML, Williams PA, et al. Raman spectroscopy of the sampleite group of minerals. J Raman Spectrosc. 2007;38(5):574–83. https://doi.org/10.1002/jrs.1702.
25. Avarcová S, Hradil D, Hradilová J, et al. Micro-analytical evidence of origin and degradation of copper pigments found in Bohemian Gothic murals. Anal Bioanal Chem. 2009;395(7):2037–50. https://doi.org/10.1007/s00216-009-3144-7.
26. Clarke RM, Williams IR. Moolooite, a naturally occurring hydrated copper oxalate from Western Australia. Mineral Mag. 1986;50(356):295–8. https://doi.org/10.1180/minmag.1986.050.356.15.
27. Twilley J, Garland K. The redecoration history of a Chinese polychromed Guanyin attributed to the 11th–12th century CE as deduced from stratigraphic microanalysis. Mater Res Soc Symp Proc. 2011;1319:231–48. https://doi.org/10.1557/opl.2011.748.
28. NIST XPS database. https://srdata.nist.gov/xps/Default.aspx/. Accessed 1 May 2022.
29. Bang S, Johnson MD, Korfiatis GP, et al. Chemical reactions between arsenic and zero-valent iron in water. Water Res. 2005;39(5):763–70. https://doi.org/10.1016/j.watres.2004.12.022.
30. Wang LL, Li ZM, Chen HL, Ma QL. Study in ploychromy decoration materials of buddhist sculpture of Sichuan and Chongqing grottoes: a case of Dazu Rock Carving on Mountain Baoding Xiaofowan Sita. Border Arch. 2017;2:385–91 (**in Chinese**).

Publisher's Note